

# THE LANCET Microbe

## **Supplementary appendix**

This appendix formed part of the original submission and has been peer reviewed.  
We post it as supplied by the authors.

Supplement to: Townsend, Hayley B Hassler, Zheng Wang, et al. The durability of immunity against reinfection by SARS-CoV-2: a comparative evolutionary study. *Lancet Microbe* 2021; published online Oct 1. [https://doi.org/10.1016/S2666-5247\(21\)00219-6](https://doi.org/10.1016/S2666-5247(21)00219-6).

## The durability of immunity against reinfection by SARS-CoV-2

### Supplementary materials

#### Contents

Investigators	02
Supplemental Figure 1	03
Supplemental Figure 2	04
Supplemental Figure 3	05
Supplemental Figure 4	06
Supplemental Figure 5	07
Supplemental Figure 6	08
Supplemental Figure 7-9	09
Supplemental Figure 10-12	10
Supplemental Figure 13	11
Supplemental Figure 14	12

## Investigators

Jeffrey P. Townsend, PhD<sup>1,2,3,4</sup>

Hayley B. Hassler, BS<sup>1</sup>

Zheng Wang, PhD<sup>1</sup>

Sayaka Miura, PhD<sup>5</sup>

Jaiveer Singh<sup>6</sup>

Sudhir Kumar, PhD<sup>6</sup>

Nancy H. Ruddle, PhD<sup>7</sup>

Alison P. Galvani, PhD<sup>2,7,8</sup>

Alex Dornburg, PhD<sup>9</sup>

<sup>1</sup>Department of Biostatistics, Yale School of Public Health, New Haven, Connecticut 06510, USA

<sup>2</sup>Department of Ecology and Evolutionary Biology, Yale University, New Haven, Connecticut 06525, USA

<sup>3</sup>Program in Computational Biology and Bioinformatics, Yale University, New Haven, Connecticut 06511, USA

<sup>4</sup>Program in Microbiology, Yale University, New Haven, Connecticut 06511, USA

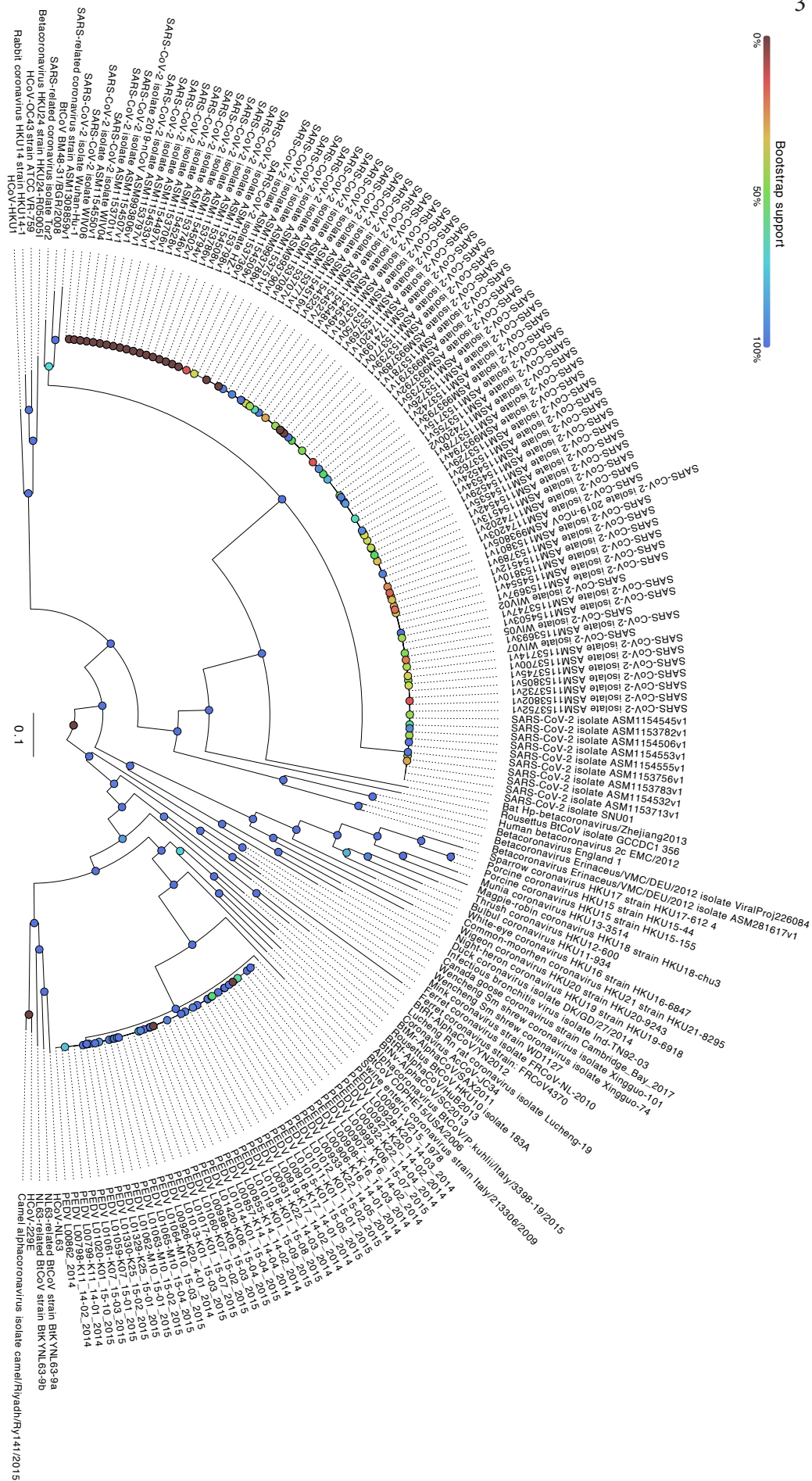
<sup>5</sup>Institute for Genomics and Evolutionary Medicine, and Department of Biology, Temple University, Philadelphia, Pennsylvania 19122, USA

<sup>6</sup>Yale College, New Haven, Connecticut

<sup>7</sup>Department of Epidemiology of Microbial Diseases, Yale School of Public Health, New Haven, Connecticut 06520

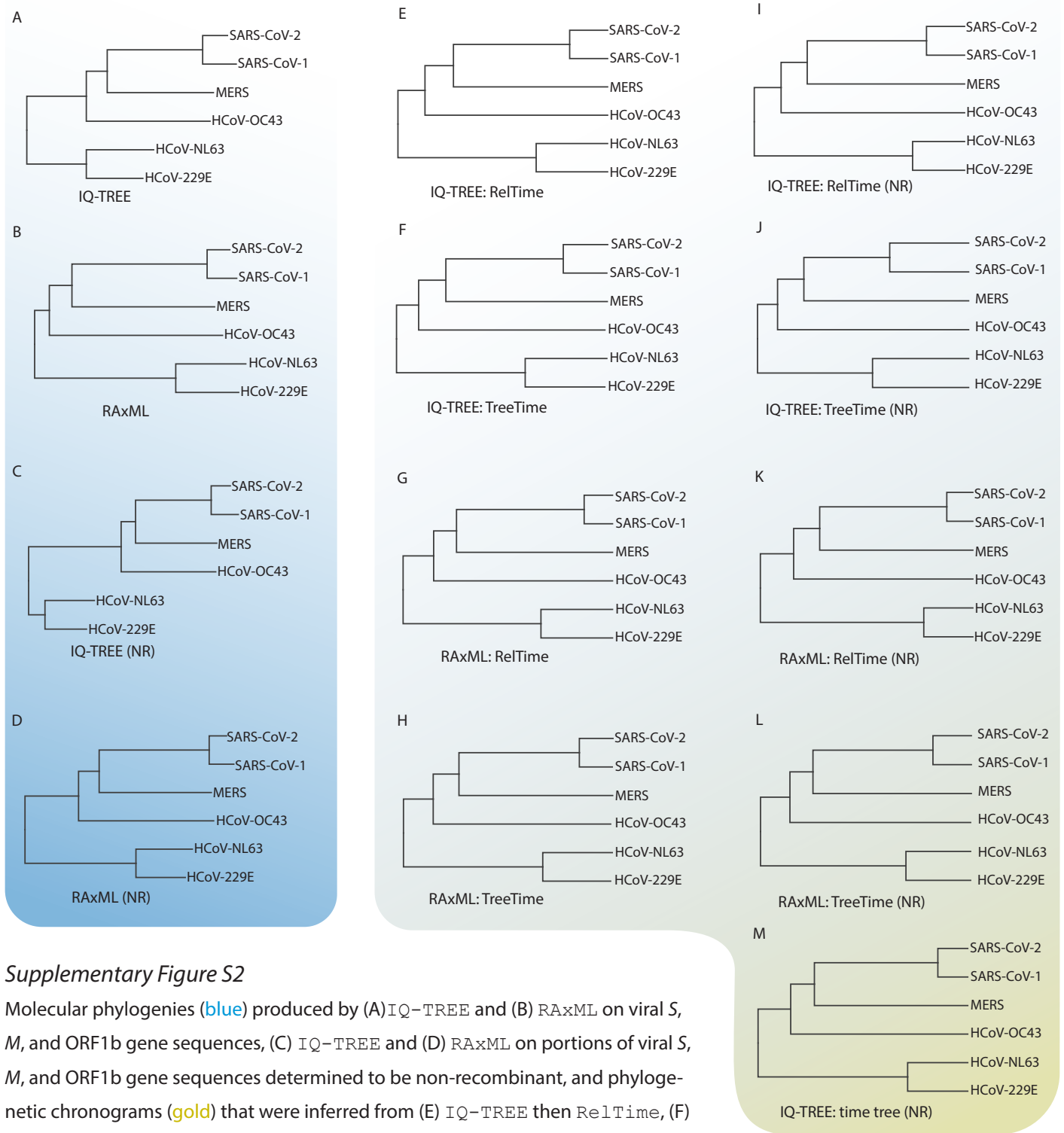
<sup>8</sup>Center for Infectious Disease Modeling and Analysis, Department of Epidemiology of Microbial Disease, Yale School of Public Health, New Haven, Connecticut 06525

<sup>9</sup>Department of Bioinformatics and Genomics, University of North Carolina, Charlotte, NC 28223



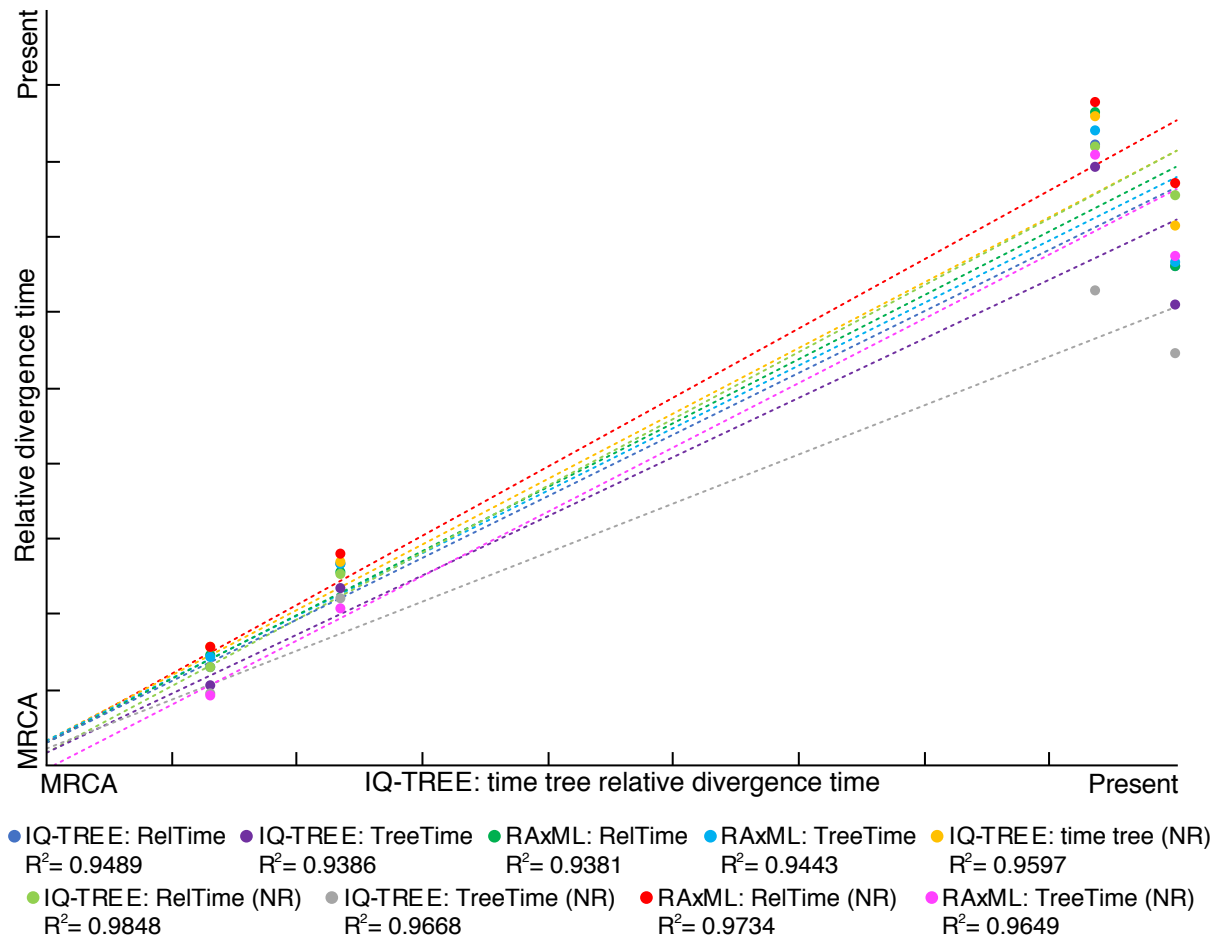
Supplementary Figure S1

Molecular phylogeny inferred using maximum likelihood<sup>7</sup> on the aligned sequences of *S*, *M*, and ORF1b genes for 58 *Alphacoronavirus*, 105 *Betacoronavirus*, 11 *Deltacoronavirus*, and three *Gammacoronavirus* taxa. Support for internodes was assessed by nonparametric bootstrap of sequence data (warm colors e.g. **red** or **orange** or **yellow**: low bootstrap support; cool colors e.g. **dark blue**: high bootstrap support).



### Supplementary Figure S2

Molecular phylogenies (blue) produced by (A) IQ-TREE and (B) RAxML on viral *S*, *M*, and ORF1b gene sequences, (C) IQ-TREE and (D) RAxML on portions of viral *S*, *M*, and ORF1b gene sequences determined to be non-recombinant, and phylogenetic chronograms (gold) that were inferred from (E) IQ-TREE then RelTime, (F) IQ-TREE then TreeTime, (G) RAxML then RelTime, (H) RAxML then TreeTime, (I) IQ-TREE then RelTime on non-recombinant sequences, (J) IQ-TREE then TreeTime on non-recombinant sequences, (K) RAxML then RelTime on non-recombinant sequence (L) RAxML then TreeTime on non-recombinant sequences, and (M) IQ-TREE on non-recombinant sequences, conditioned on the evolutionary divergences of human-infecting coronaviruses. Bootstrap support was 100% for all nodes of these phylogenies. NR: Based on viral gene sequences that were determined to be non-recombinant.



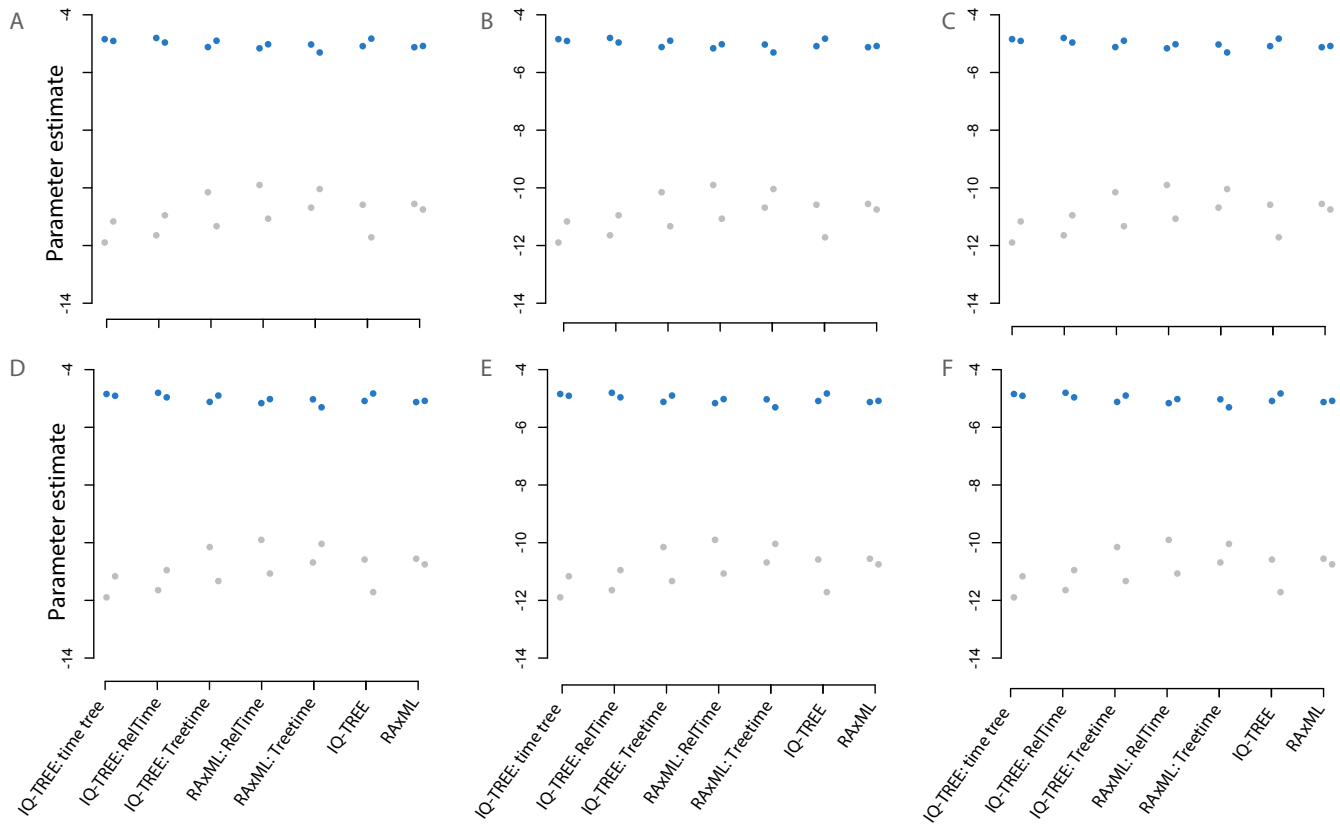
### Supplementary Figure S3

Scatter plot of the node ages estimated by phylogenetic chronograms derived from IQ-TREE and RAxML molecular phylogenies compared to the IQ-TREE estimated divergence times. NR: Based on viral gene sequences that were determined to be non-recombinant.

Molecular divergences		Sars-CoV-1	HCoV-HKU1	HCoV-NL63	MERS	HCoV-OC43	HCoV-229E	
		21.8 %	55.0 %	55.3 %	55.4 %	57.4 %	78.0 %	<i>Sars-CoV-2</i>
<i>Sars-CoV-1</i>	0.16		56.2 %	56.6 %	55.8 %	57.7 %	78.6 %	<i>Sars-CoV-1</i>
<i>HCoV-HKU1</i>	0.87	0.87		55.2 %	57.1 %	40.6 %	78.2 %	<i>HCoV-HKU1</i>
<i>HCoV-NL63</i>	1.0	1.0	1.0		58.9 %	57.1 %	74.5 %	<i>HCoV-NL63</i>
<i>MERS</i>	0.76	0.76	0.87	1.0		57.5 %	80.1 %	<i>MERS</i>
<i>HCoV-OC43</i>	0.87	0.87	0.33	1.0	0.87		79.4 %	<i>HCoV-OC43</i>
<i>HCoV-229E</i>	1.0	1.0	1.0	0.10	1.0	1.0		
	<i>Sars-CoV-2</i>	<i>Sars-CoV-1</i>	<i>HCoV-HKU1</i>	<i>HCoV-NL63</i>	<i>MERS</i>	<i>HCoV-OC43</i>	Relative Divergence times	

### Supplementary Figure S4

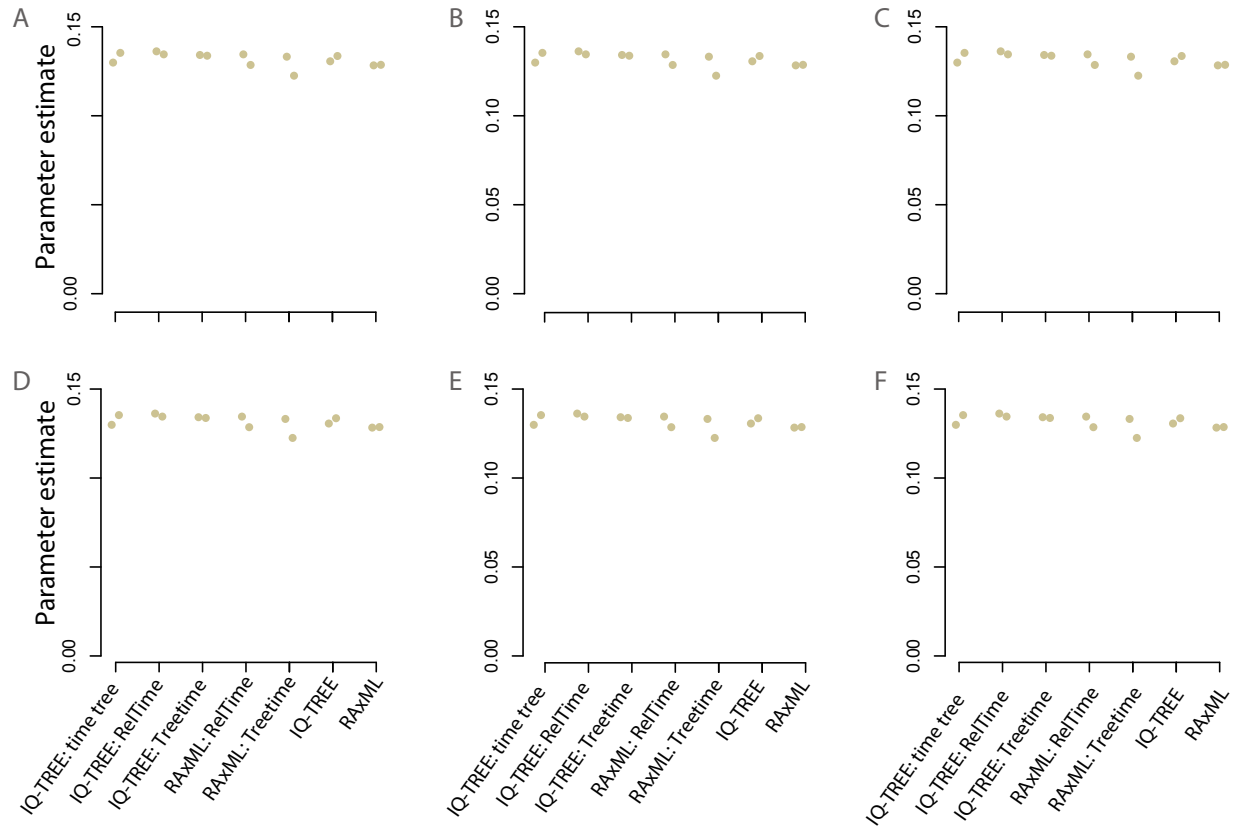
Viral percent sequence divergences (blue; based on the alignment of the *S*, *M*, and ORF1b genes), and estimated pairwise divergence times (beige; from our IQ-TREE phylogenetic chronogram analysis, with time calibrated relative to the MRCA at 1.0).



### Supplementary Figure S5

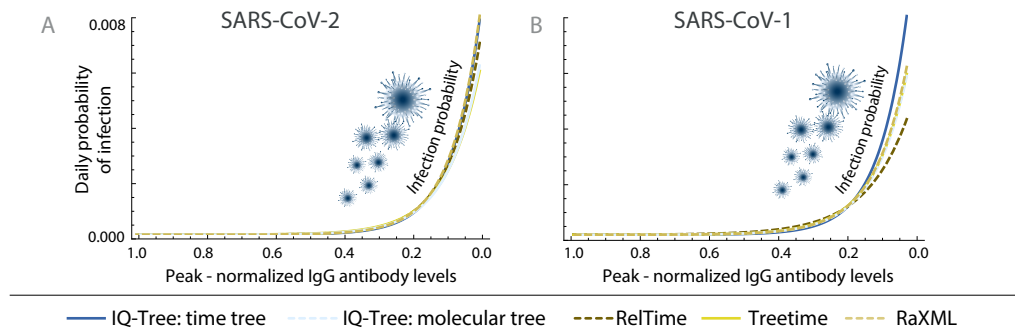
Evaluation of the sensitivity of the `Rphylopar` estimate based on A) anti-N IgG; B) anti-S IgG; C) anti-whole-virus IgG; D) an alternate data source for SARS-CoV-1 anti-N IgG; E) an alternate data source for MERS-CoV anti-S IgG; and F) an alternate data source for anti-whole virus IgG to the slope ( $b$ , blue) and intercept ( $a$ , gray) parameters for the logistic regression function, as they depend on molecular divergence phylogenies or phylogenetic chronograms generated via several common approaches to phylogenetic inference.





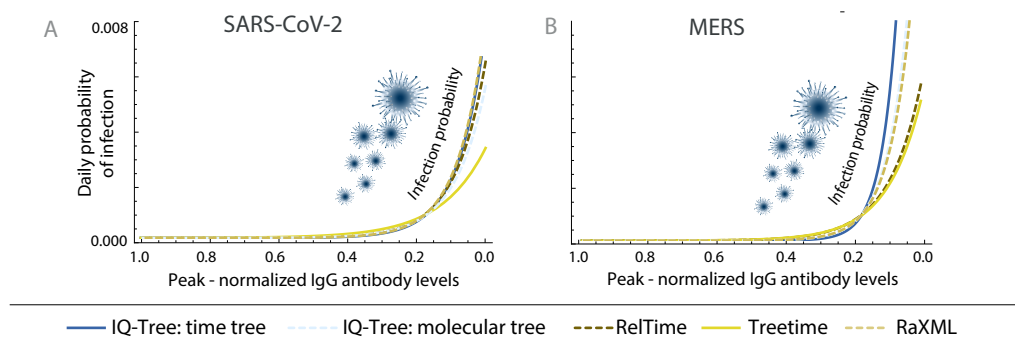
### Supplementary Figure S6

Evaluation of the sensitivity of the `Rphyloparse` estimate based on A) anti-N IgG; B) anti-S IgG; C) anti-whole-virus IgG; D) an alternate data source for SARS-CoV-1 anti-N IgG; E) an alternate data source for MERS-CoV anti-S IgG; and F) an alternate data source for anti-whole virus IgG to the baseline parameter for the logistic regression function, as they depend on molecular divergence phylogenies or phylogenetic chronograms generated via several common approaches to phylogenetic inference.



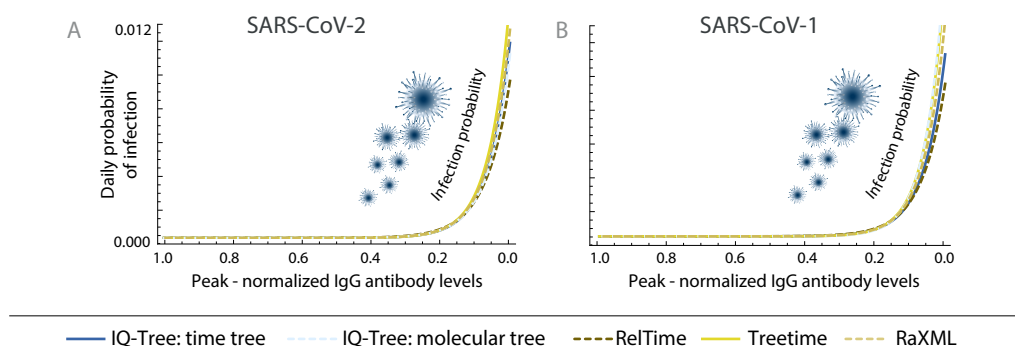
### Supplementary Figure S7

Evaluation of the sensitivity of the *Rphylopars*-based estimation of the relationship between the daily infection probability and the peak normalized anti-N protein Immunoglobulin G antibody levels for A) SARS-CoV-2 & B) SARS CoV-1 as they depend on molecular divergence phylogenies or phylogenetic chronograms generated via several common approaches to phylogenetic inference. Anti-N IgG data was not available for MERS-CoV.



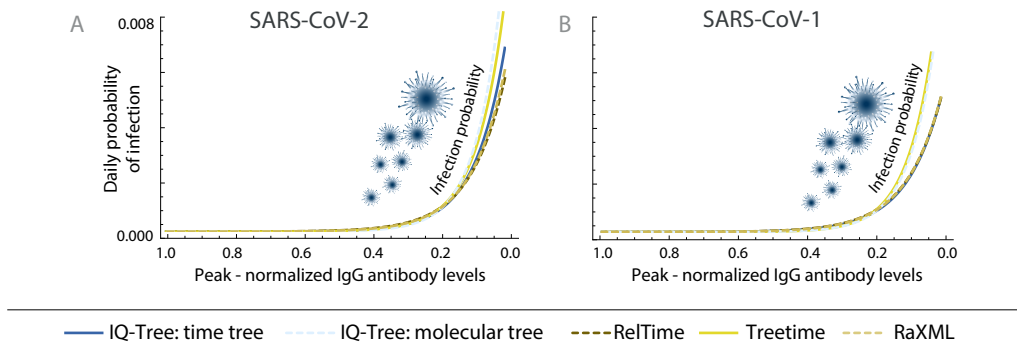
### Supplementary Figure S8

Evaluation of the sensitivity of the *Rphylopars*-based estimation of the relationship between the daily infection probability and the peak normalized anti-S-protein Immunoglobulin G antibody levels for A) SARS-CoV-2 & B) MERS-CoV as they depend on molecular divergence phylogenies or phylogenetic chronograms generated via several common approaches to phylogenetic inference. Anti-S IgG data was not available for SARS-CoV-1.



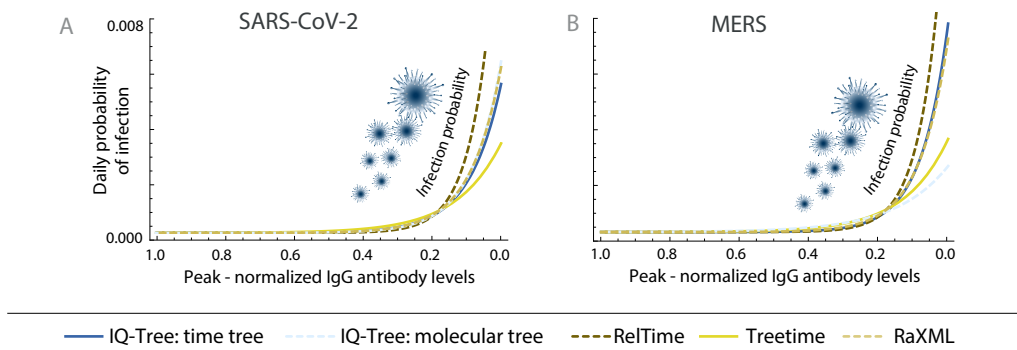
### Supplementary Figure S9

Evaluation of the sensitivity of the *Rphylopars*-based estimation of the relationship between the daily infection probability and the peak normalized anti-whole virus Immunoglobulin G antibody levels for A) SARS-CoV-2 & B) SARS CoV-1 as they depend on molecular divergence phylogenies or phylogenetic chronograms generated via several common approaches to phylogenetic inference. Anti whole-virus IgG data was not available for MERS-CoV.



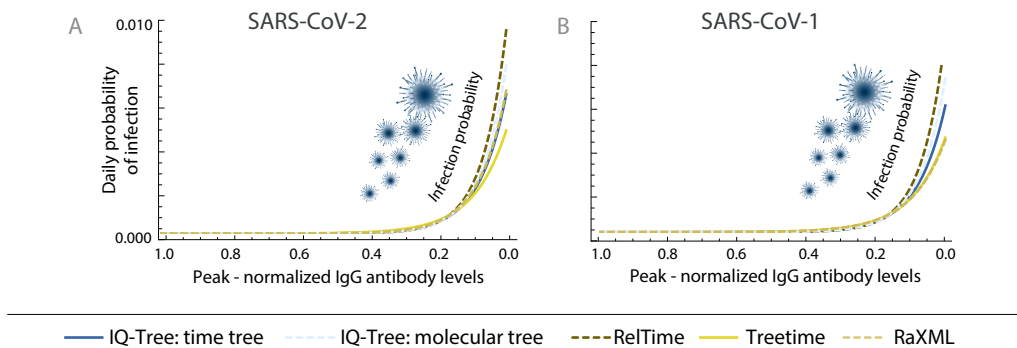
### Supplementary Figure S10

Evaluation of the sensitivity of the *Rphylovars*-based estimation of the relationship between the daily infection probability and the peak normalized anti-N protein Immunoglobulin G antibody levels using an alternate data source for SARS-CoV-1 as they depend on molecular divergence phylogenies or phylogenetic chronograms generated via several common approaches to phylogenetic inference. Anti-N IgG data was not available for MERS-CoV.



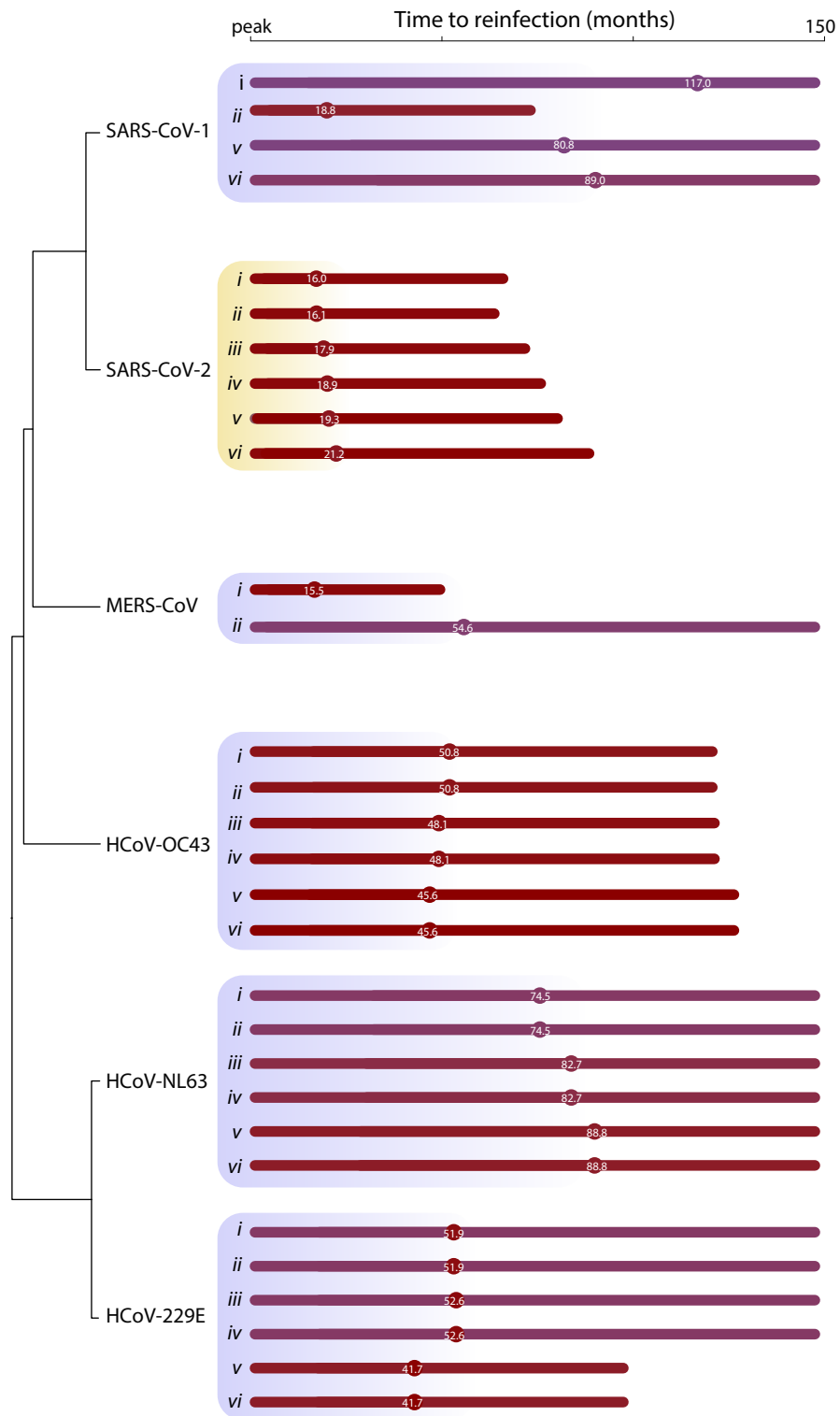
### Supplementary Figure S11

Evaluation of the sensitivity of the *Rphylovars*-based estimation of the relationship between the daily infection probability and the peak normalized anti-S-protein Immunoglobulin G antibody levels A) SARS-CoV-2 & B) MERS-CoV using an alternate data source for MERS-CoV as they depend on molecular divergence phylogenies or phylogenetic chronograms generated via several common approaches to phylogenetic inference. Anti-S IgG data was not available for SARS-CoV-1.



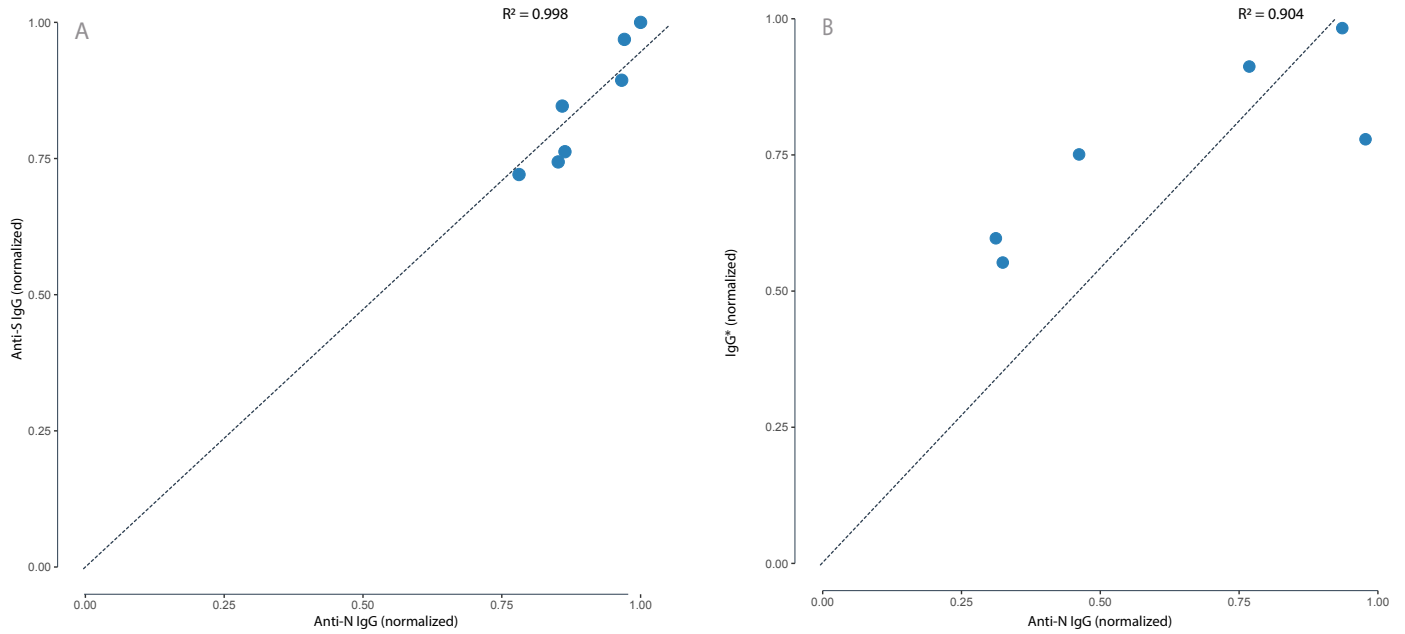
### Supplementary Figure S12

Evaluation of the sensitivity of the *Rphylovars*-based estimation of the relationship between the daily infection probability and the peak normalized anti-whole-virus Immunoglobulin G antibody levels from an alternate data source for SARS-CoV-1 for A) SARS-CoV-2 & B) SARS-CoV-1 as they depend on molecular divergence phylogenies or phylogenetic chronograms generated via several common approaches to phylogenetic inference. Anti-whole-virus IgG data was not available for MERS-CoV.



*Supplementary Figure S13*

Evaluation of the sensitivity of the times to reinfection for each coronavirus resulting from analyses of datasets i–vi (detailed in the Fig. 1 legend), in days from peak antibody level at 3 months.



### Supplementary Figure S14

Results of a linear regression demonstrating the relationship between (A) normalized anti-N IgG and normalized anti-S IgG levels ( $P = 6.63 \times 10^{-9}$ ) and (B) normalized anti-N and normalized anti-virus lysate IgG levels ( $P = 0.000623$ ) at the same time points. Dotted line indicates the expectation of linear model fit through the origin.